

(NASA-CR-176864) A DENSITOMETRIC ANALYSIS
OF IIAO FILM FLOWN ABOARD THE SPACE SHUTTLE
TRANSPORTATION SYSTEM STS-3, STS-8, AND
STS-7 Semiannual Report, Dec. 1986 (Morgan
State Univ., Baltimore, Md.) 23 p CSCL 14E G3/35

N86-31858

Unclas
43552

IN-26412

A DENSITOMETRIC ANALYSIS OF IIAO FILM FLOWN ABOARD
THE SPACE SHUTTLE TRANSPORTATION SYSTEM STS-3, STS-8, & STS-7

SEMI-ANNUAL REPORT
December, 1986

NSG-5074

BY

Ernest C. Hammond Jr., Kevin A. Peters, Pamela F. Atkinson

MORGAN STATE UNIVERSITY
BALTIMORE, MARYLAND 21239

Submitted to NASA, Laboratory for Astronomy and Solar Physics,
Goddard Space Flight Center, Greenbelt, Maryland 20770

Ernest C. Hammond, Jr.
Morgan State University
Baltimore, Maryland 21239

Slide (2), Slide (3) 11aO film for this experiment was obtained from the same roll of Kodak Film Mfg. date 5-76-A5J. The film was loaded into specially prepared aluminum anodized packages that would fit aboard the Space Shuttle's Getaway Special Container. One roll of film was cut from the same stock and maintained as the control. The control film was maintained at a temperature of 22 degrees °C at Goddard Space Flight Center. After the mission, the three rolls of 11aO film were shipped back to the Small Payload Section of the Laboratory for Astronomy and Solar Physics. One film and the control were developed as Set I, while the other 11aO sample film was developed as Set II, Samples A and B.

Using MacBeth Densitometer, measurements were obtained from the film every 2 centimeters, developing 3 columns of data. Slide (4) Significant differences were found when samples were compared with the control. Sample A and Sample B had a 5.26% increase in density or fogging background, while the film developed shortly after its arrival at Goddard Space Flight Center displayed a 3.8% increase in the density or the fogging background.

Slides (5,6,7) An analysis of the data for each sample film aboard the Space Shuttle indicates variation in intensity with respect to the fogging levels as a function of position on the film. There is a tendency of more random variation toward one end of the film, but the actual orientation in the Space Shuttle is unknown. A possible theory is that the high energy cosmic rays had penetrated the aluminum film cartridges aboard the Space Shuttle causing certain secondary reactions that produce variations toward one end of the film due to the wrapping procedure used in the placement of the film in the canister. Other theories suggest thermal effects cause density variation, it is known that aluminum containers tend to innately fog various UV films along with the wrapping geometry of the film within the canister.

DENSITOMETRIC RESPONSE OF 11aO FILM FLOWN ON STS-7.

Three canisters of 35mm 11aO film were flown on STS-7 in a getaway special canister in cooperation with NASA's Plasma Physics Branch and the Naval Research's Solar Astronomy Branch. The results indicate a high degree of thermal aging while aboard and during the space shuttle mission.

been developed at the same time as the flight film received from STS-7.

EXPERIMENTAL SET UP FOR STS-8

This research team was able to use one of the canisters to place four rolls of film on STS-8, one roll of Ilford G5 nuclear emulsion, and one roll of a new batch of Ilford. The Naval Research Laboratory group was using a very sensitive ultra violet film to study the effects of space on the ultraviolet emulsions. The shuttle orbit was low enough to expect some minimum cosmic ray damage to the film as well as tracks on the nuclear emulsion film. Slide (9) The Getaway Special was aligned in the bay of the shuttle with bay portals pointed to the earth for cooling purposes as shown in the figure. Slide (8)

The temperature profiles for STS-7 and STS-8 are very similar, going from a temperature of approximately 23 degrees Centigrade before launch to a temperature of approximately -22 degrees Centigrade during the flight. This temperature differentiation is sufficient to cause unusual density increases in the wedges. The major differences between STS-7 and STS-8 occurred because STS-7 had to land in California where the automatic temperature control devices and appropriate air conditioning units for the shuttle cargo were not present. Please note that once the shuttle had landed, one can measure the diurnal temperature variations. Slide (8). Terrestrial experiments have shown that less dense wedges produce densitometric increases as the temperature increases. Slide (12) over a number of days. The diagram shows the effect of the first 3 step wedges including the aging effect of the background at 32 degrees. The lowering of the temperature decreases the slope of the family curves for each of the darker step wedges. Slide (12 & 14) (aging effects) shows the slope variation at 21 degrees and at 32 degrees over a 90 day period. A most interesting effect occurs at the darker patterns. They tend to drop in density, while the lighter patterns tend to increase in density. Furthermore, the Ilford film seems to perform nonlinearly for temperature values above 67 or 68 degrees. Slide (13) The least dense step wedges tend to show dramatic increases in density above 68 degrees °C while the darker wedges show a reduction of temperature above 70 degrees. The slopes of these films is increased further when the ambient temperatures seem to increase. Slide (8)

A brief examination of the aging effects will assist us in understanding the observed effects of the film caused by the exposure to the space environment of the shuttle. Slide (14) We used a microdensitometer to contrast and compare the terrestrial film as well as the shuttle flight film. Slide (15) Using this technique we are able to calculate the signal to noise ratio for flight as well as for control film. On board STS-7 the signal to noise ratio increased while the control film decreased. The signal noise ratio computed for STS-7 shows that at higher exposure the signal to noise ratio is less than the flight film Slide (16). But at lower exposures the control and flight film seem to have larger signal to noise ratio. Slide (17) This difference may be caused by additional thermal activity within the canister as shown on Slide (17) and the lack of appropriate air conditioning equipment at the California landing site, due to bad weather at Cape Kennedy.

SIGNALS TO NOISE OF AGING FILM

Analysis of the the signals to noise ratio for 11a0 film aged 8, 19, 21, 17, and 71 days indicate that a certain amount of aging reduces the signals to noise ratio over the short term, but will increase the signal to noise ratio over the long period of time Slide (18).

An examination of the interaction of protons of varying dosage and energies indicate that the very light wedges are very sensitive to proton interaction with the emulsion while the very dark patterns tend to be less sensitive to very high MEV protons. Slide (19) and Slide (20) MEV vs. dosage were obtained by using the Harvard University Cyclotron.

Slide (18) Using the Harvard University Cyclotron, we bombarded the 11a0 film with alpha particles, searching for parallel interactions in the space shuttle due to cosmic rays as from the cyclotron. We bombarded the 11a0 film using the alpha particles there, at 47 MEV, 79 MEV, and 153 MEV for the 6.8 rad dosage. Therefore, we were hoping to see similar results when we examined the films from the shuttle.

Slide (19) But we did not. There is a differentiation during the front part of the curve, but the toe and the shoulders did not seem to respond, as a result we did not think that there was any, dramatic cosmic ray activity: Slide (20A)

MICRODENSITOMETRIC ANALYSIS

Comparing similar step wedges that have been aged from 3 to 71 days, one can immediately see an increase in granularity. Slide (21) and Slide (22) however this is not consistent for all step wedges as it is for the middle wedges. The denser the wedges, the more one observes the converse of less granularity. Slide (23) Furthermore, as aging occurs, granular definition between step wedges seems to decrease, while other step wedges under densitometric aging will produce a heavier granularity indicative of increased grain structure.

MICRODENSITOMETRIC COMPARISON OF CONTROL VS. FLIGHT FILM

Note that the control film on STS-8 for step wedges 3 has larger grain structure than the flight film. Similarly on STS-8 strip 4, a new batch of 11aO film indicates a slight increase of granularity toward the darker wedges. Slide (24) Conversely, the least dense step wedge controls are heavier than the traces for the flight film. Slide (25) Microdensitometric traces of step 4 and strip 4 tend to illustrate very small changes. Finally, traces from STS-8 again show greater granularity for the flight film than for terrestrial controls. Slide (27)

A new approach to the examination of the 11aO Film Emulsion is the use of the Scanning Electron Microscope to investigate surface grains and their structure. Varying the voltage of the probe electrons, we are able to examine grain structure under the surface of the emulsion at the proper accelerating voltage of the electrons. All the 11aO films were coated using gold palladium and standard sputtering techniques.

Slide (27) Using about 1,000 Magnification it became very evident that the energy of the electrons within the scanning electron microscope striking the emulsion is very crucial in terms of the viewing of the grain structure. What we want to do in the future is to look at the aged film and see exactly how these grains change. Slide 28

We find that a working voltage for SEM ISI SS 40 somewhere between 2 kilovolts and 10 kilovolts is sufficient to produce clear images without flaring. This flaring of the image from the SEM produces a 4-8% increase in the total area of the grain under investigation from direct measurements of the microphotograph.

Slide (29) But as the energy of the electrons increases, one notices that there is a flare effect, each grain spreading out brightly. Then you begin to see some of the grains beneath the surface of the emulsion. So, using this scanning electron technique, we can examine some of the grains just below the surface if the charging voltage is proper.

Slide (31) Here again is one at 20 kilovolts, and you can see the flaring of each of the grains of the IlaO.

Slides (33, 34, 35, and 36A & B) One of the interesting things that we attempted to do was to look at the wedges that we have had, and to put them under the electron microscope. The extreme left represents the least dense, and the extreme right would represent the most dense. Of course, as the density increases, the size of these grains seems to decrease. Using this technique, one can measure with ease; and get some sort of statistical handle on what is happening there. Slides (38).

Using energy dispersive qualitative analysis techniques reveals a very large silver peak along with traces of copper sodium and sulfur and argon peaks as shown in Slide (38). These trace element peaks are associated with the elements used in the development process and other materials in the emulsion.

RECIPROCITY FAILURE OF IlaO FILM

Reciprocity Failure was examined for IlaO spectroscopic film. The failure was examined over two ranges of time from one second to thirty-one seconds and one minute to 180 minutes. The variation to illuminance was obtained by using thirty neutral density filters. A standard sensitometric device imprinted the wedge pattern on the film as exposure time was subjected to variation. The utilization of IlaO film is recommended for low illumination, producing small reciprocity failure effects which is predicted by the manufacturer. Our results indicate reciprocity failure occurring for higher density patterns within the first minute. Multiple failure occurs at 13, 30, 80, and 180 minutes.

Ernest C. Hammond, Jr.
Morgan State University
Baltimore, Maryland 21239

MATERIALS AND METHODS

Twenty-seven wedge patterns were placed on 11a0 spectroscopic film, in total darkness, using a light sensitometer, with a 24 hour burn in time for the bulb. Each film section was exposed to the light sources for a specific period of time. Time intervals were the following: 1-30 seconds and 1-11, 15, 19, 22.5, 25, 27, 30, 35, 40, 45, 58, 90, 125, and 180 minutes, respectively.

The film was then developed using Kodak D-19 developer, rapid fixer, hypo-clearing agent and photoflo solutions. The following development procedure was used for each film section: In absolute darkness, and a water bath at a temperature of $20^{\circ}\text{C} + 1.5^{\circ}\text{C}$, one section of film was placed in Kodak D-19 developer and gently agitated for four minutes using a specific soak and agitating pattern. It was washed in water for 30 seconds, shaken, then placed in Kodak rapid fixer solution, using the exact same pattern of agitation and soaking, and gently agitated for four minutes. It was then removed, rinsed in water for 30 seconds, washed in water for 30 seconds, placed in photoflo-flo solution (1:200 dilution) for one minute, then hung to dry. After development, the optical densities of the wedge patterns were read using a MacBeth Densitometer.

INTRODUCTION

With NASA's Ultraviolet Imaging Telescope, (UIT), the space telescope of the consortium of universities, and other ultraviolet experiments being conducted by the University of Wisconsin and others, it becomes an absolute necessity that an in depth examination of the phenomena reciprocity failure using the primary photographic material - 11a0 film - be analyzed before utilization on the space shuttle or terrestrial observatories.

RESULTS

An examination of the reciprocity failure for the 1 to 30 second exposure periods (i.e., a separate wedge pattern was exposed to an amount of light from 1 to 30 seconds sequentially) reveals that for two separate batches of film whose history of use was different, there is some Reciprocity Failure occurring at the darker wedge patterns. Slides (39,40,41,42,

Ernest C. Hammond, Jr.
Morgan State University
Baltimore, Maryland 21239

SUMMARY

The results of these studies have implications for the utilization of the IlaO spectroscopic film on the future shuttle and space lab missions. These responses to standard photonic energy sources will have immediate application for the uneven responses of the film photographing a star field in a terrestrial or extraterrestrial environment with associated digital imaging equipment.

The author is indebted to Gerry Baker and Al Stober of the Small Payloads Section of the Laboratory for Solar Physics and Astronomy for their hours of discussion and support. Special thanks to Dr. Dan KlingleSmith of the Interactive Astronomical Data Analysis Facility also of the Goddard Space Flight Center, Greenbelt, Maryland for his patient assistance during the imaging processing of these films. Very special thanks to Kevin Peters, Sean Gunther, Lisa Cunningham, and Deborah Wright for their careful assistance during the development process.

Ernest C. Hammond, Jr.
Morgan State University
Baltimore, Maryland 21239

and 43) While an examination of the very light patterns further shows the trend of reciprocity failure at the 30th and 31st seconds. It should be noted that the very darkest patterns have a marked decrease in reciprocity failure around the 30 second interval, with other variations occurring at 10, 15, and 19 seconds consistently with each variation of the pattern. Slides (44, 45, 46, 47, and 48)

An examination of Reciprocity Failure for the time period of exposure from 1 to 3 hours shows five minimum points where reciprocity failure occurs. The Reciprocity Failure minimum points occur at 13 minutes, 20 minutes, 30 minutes, and 90 minutes, with a less defined failure at ± 80 minutes. The middle density wedges indicate the same reciprocity failure points occurring at the same time. The darkest wedges show remarkable stability for the first 10 minutes exposure, but dramatic failures occur at 11 minutes, and 20 minutes. Very dramatic reductions occur at 30 minutes.

CONCLUSION

For exposure times of 30 to 31 seconds, darker wedges experience failure more than light wedge patterns. This indicates that the lighter wedges are less sensitive to Reciprocity Failure at short exposure times. As the exposure time increases, there appears to be some migration of grains in the darker wedges; especially the last three columns which gave an appearance that a double exposure had occurred. There is also an increased darkening of the film with increased exposure times. Fogging of the film is prevalent at 30, 45, 58, 90, and 180 minutes, again with increased exposure times. An examination of the reciprocity failure from 1 to 180 minutes completely demonstrates the following: (a) The Reciprocity Failure minimum points are at 13 minutes, 20 minutes, 30 minutes, and 90 are at and less defined failure occurs at 11 minutes. The light and middle density wedges showed this evidence. Darker wedges (b) show remarkable stability for the first 10 minutes of exposure, but reductions at 11 minutes, 20 minutes, and dramatic reductions at 30 minutes.

ORIGINAL PAGE IS
OF POOR QUALITY

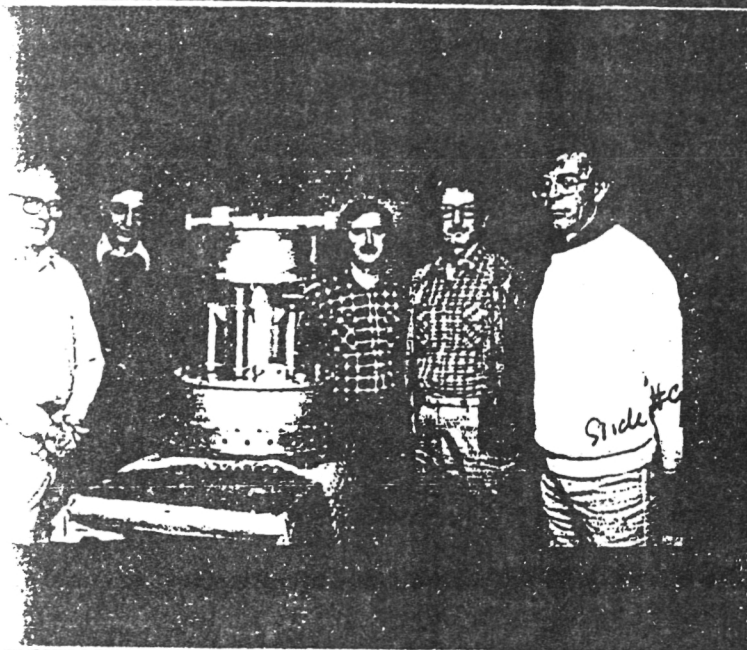
Session # 2

Talk # 4

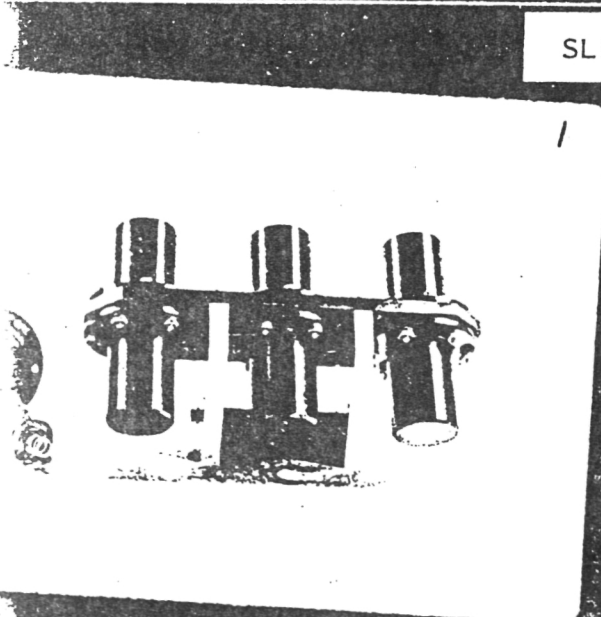
Hammond

Slide A

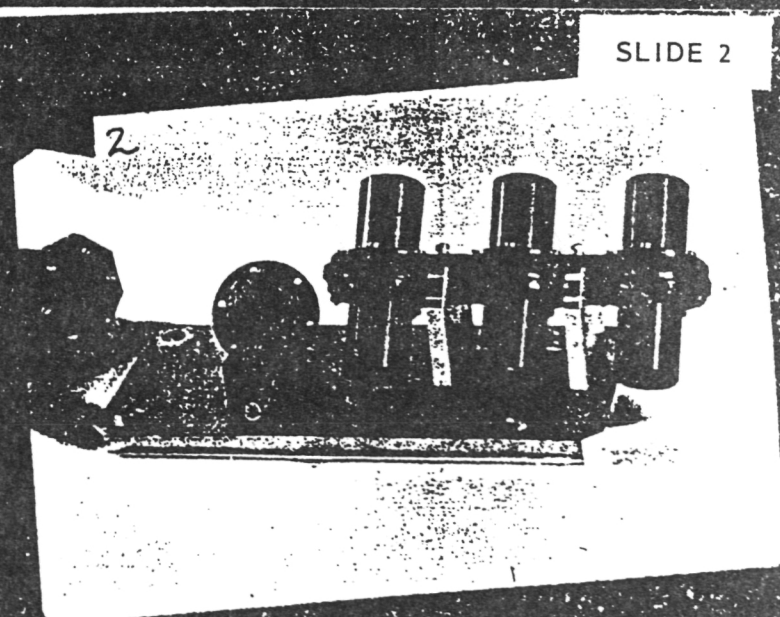
SLIDE A



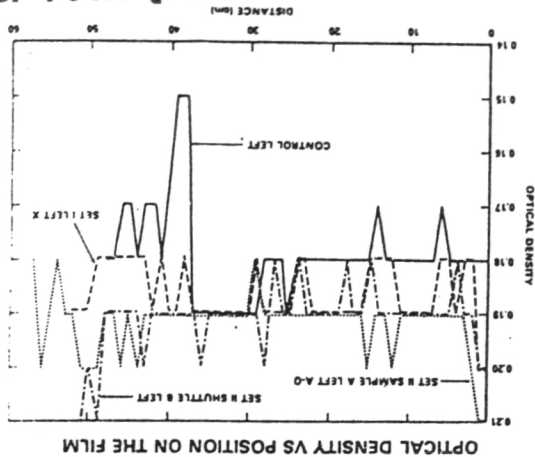
SLIDE 1



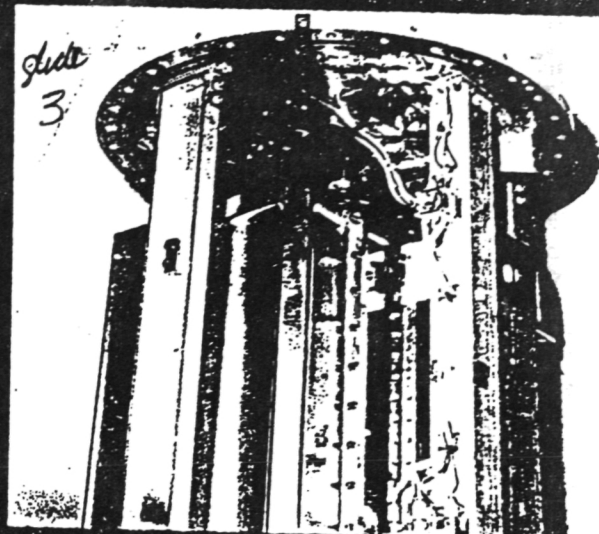
SLIDE 2



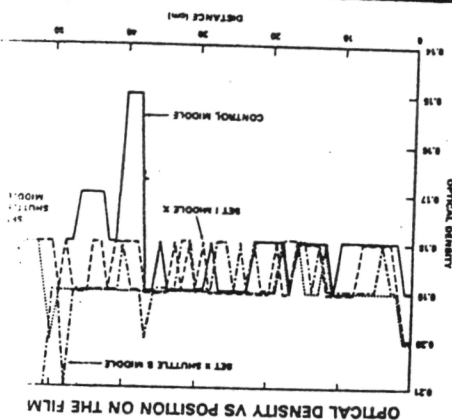
SLIDE 7



Slide 7

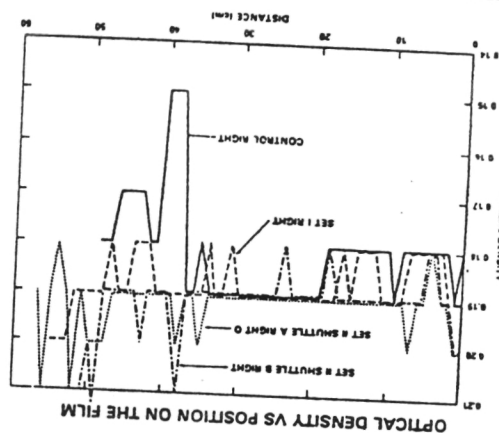


SLIDE 6



Slide 6

SLIDE 5



Slide 5

SLIDE 4

Shuttle Set Sample A & B

	LEFT	MIDDLE	RIGHT
Shuttle Set Sample A	.23%	.41%	.10%

Slide 4

% DIFFERENCE BETWEEN SHUTTLE SET A & B

CONTROL VS

SHUTTLE SET 1

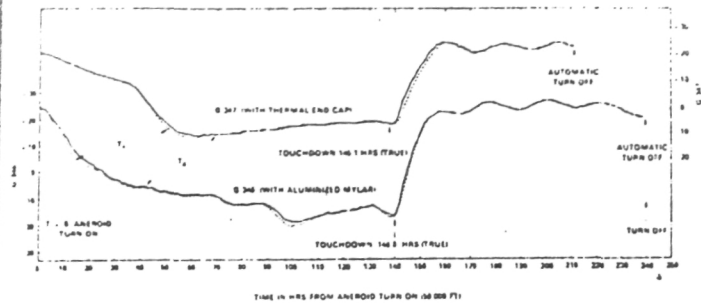
SHUTTLE SET A

SHUTTLE SET B

TOTAL SHUTTLE SAMPLES

SLIDE 8

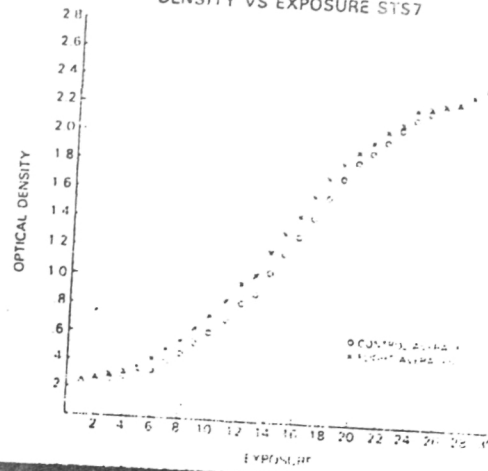
TEMPERATURE PROFILES FOR
G 346 LAUNCHED 5:18:53 1130 GMT
G 347 LAUNCHED 9:30:53 0632 GMT



Slide 8 Slide 8

SLIDE 8

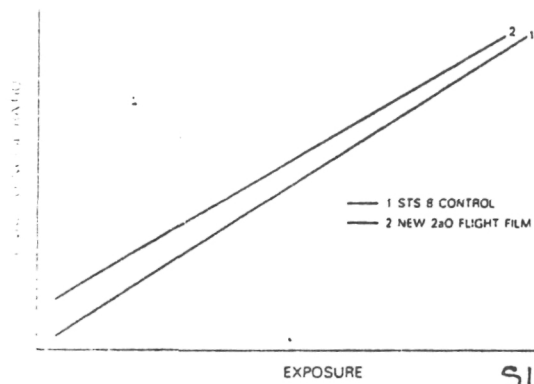
DENSITY VS EXPOSURE STS7



Slide #8

SLIDE 15

SIGNAL TO NOISE STS8

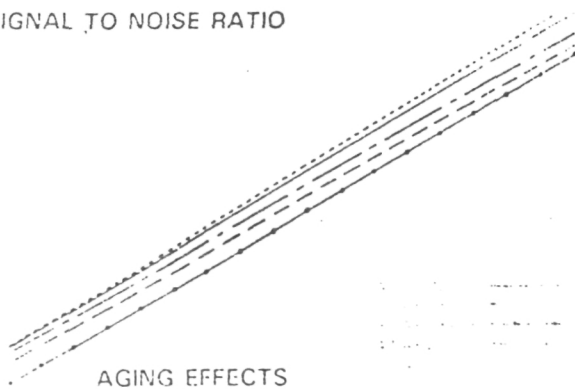


Slide #15



SLIDE 18

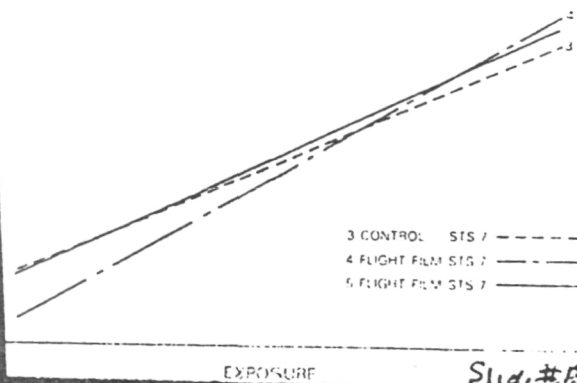
SIGNAL TO NOISE RATIO



Slide #18

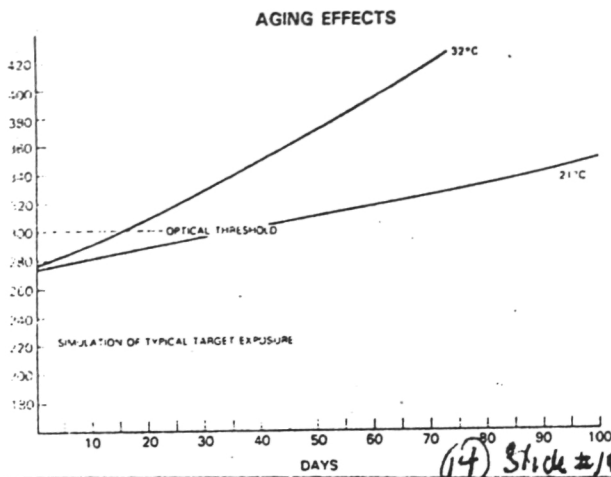
SLIDE 16

SIGNAL TO NOISE RATIO STS7

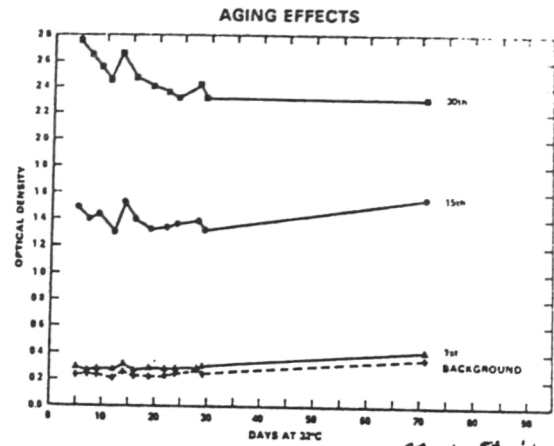


Slide #16

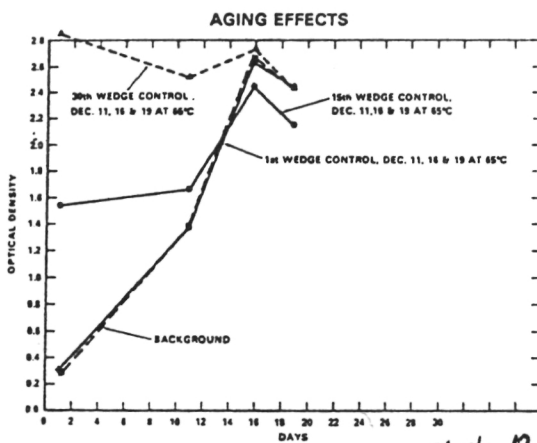
SLIDE 14



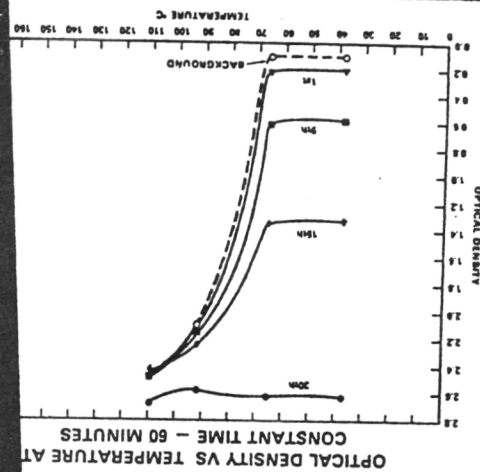
SLIDE 12



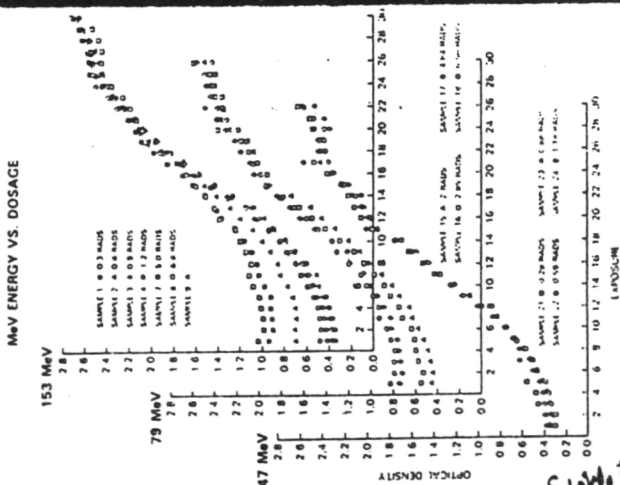
SLIDE 11



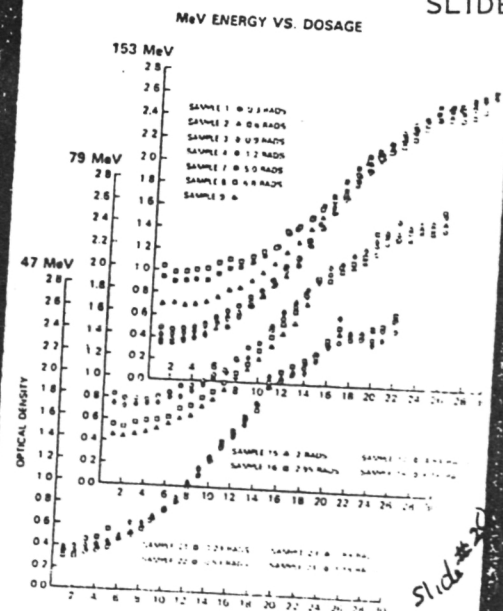
SLIDE 13



SLIDE 19

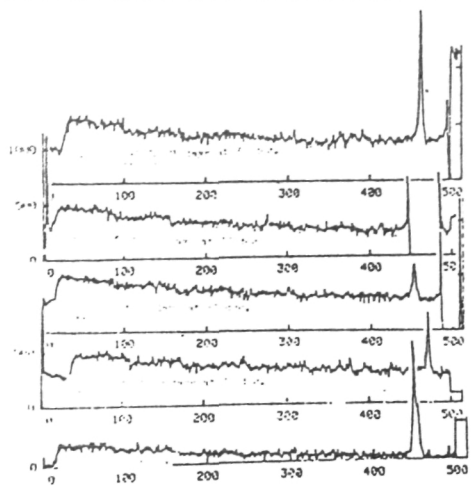


SLIDE 20



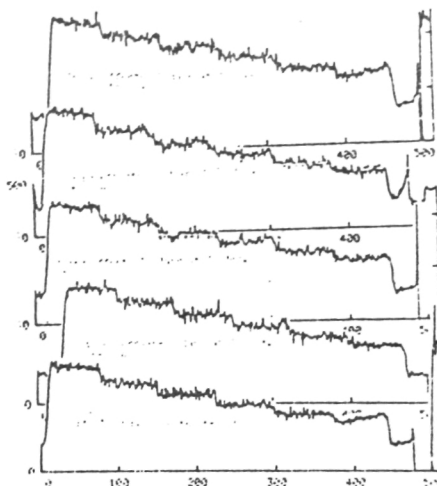
ORIGINAL PAGE IS
OF POOR QUALITY

SLIDE 22

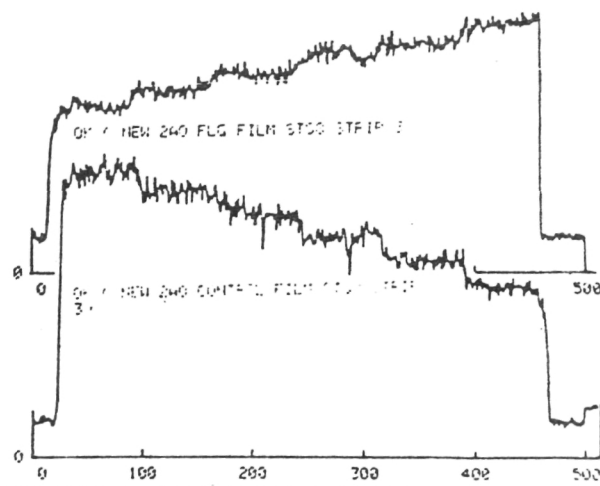
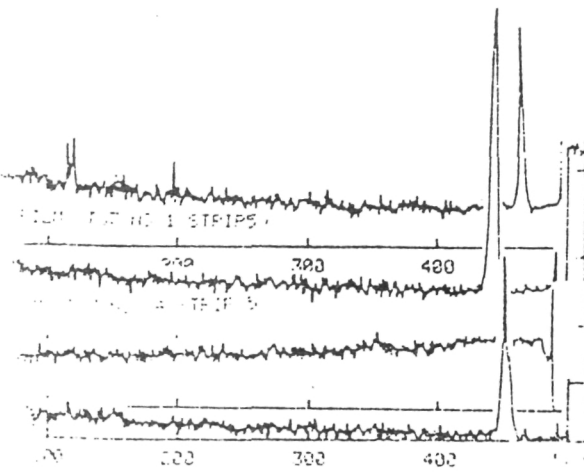


Slide 22

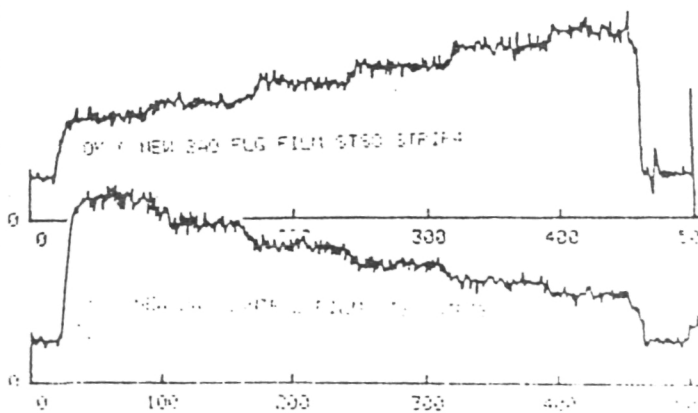
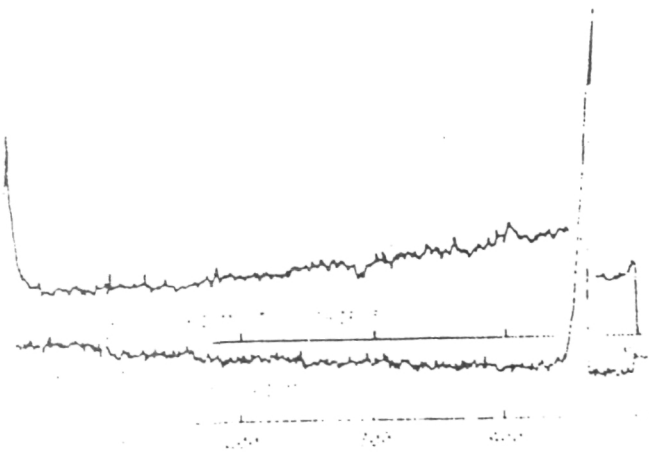
SLIDE 21



Slide 21



SLIDE 24



Slide 24

SLIDE 26

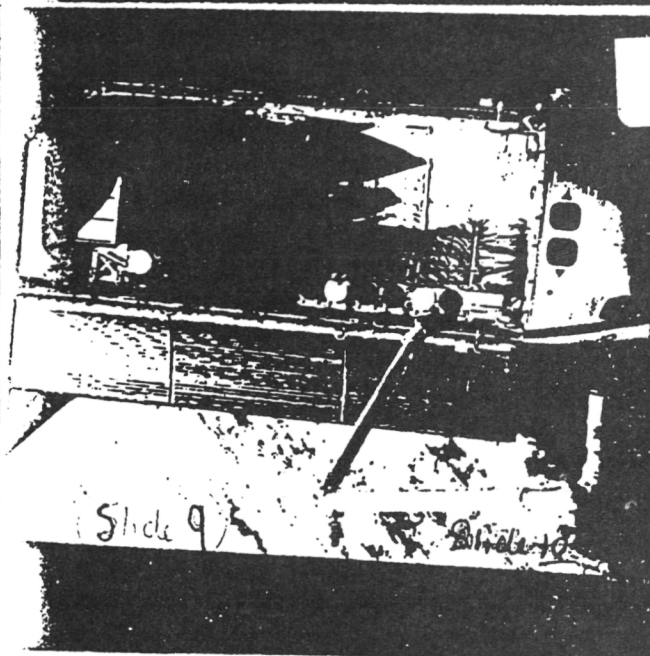
10mm 37KU 137ES 2332-88 PHILIP

ORIGINAL PAGE IS
OF POOR QUALITY

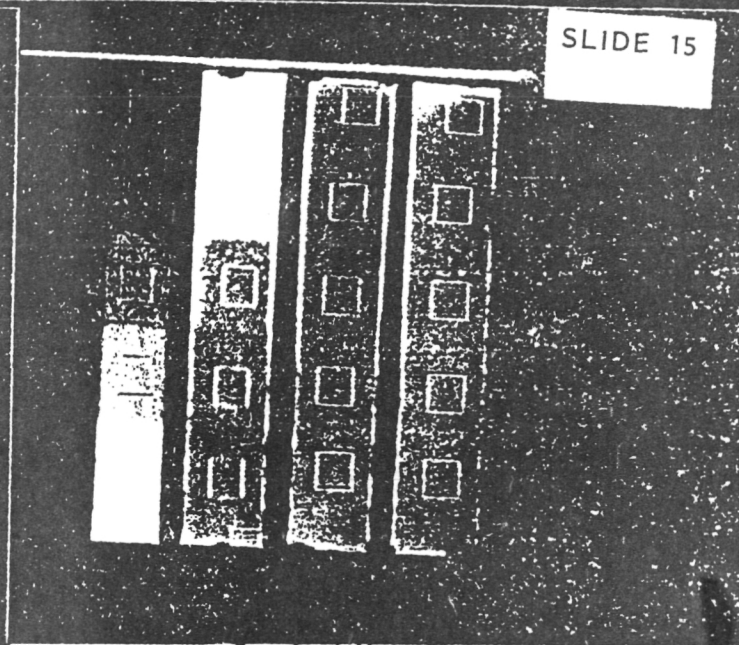
CONTROL vs TOTAL DENSITY % DIFFERENCE

	LEFT	MIDDLE	RIGHT
Shuttle Set I	5.11%	3.36%	2.67%
Shuttle Set A	6.76%	4.73%	4.73%
Shuttle Set B	6.52%	4.30%	4.62%

SLIDE 9

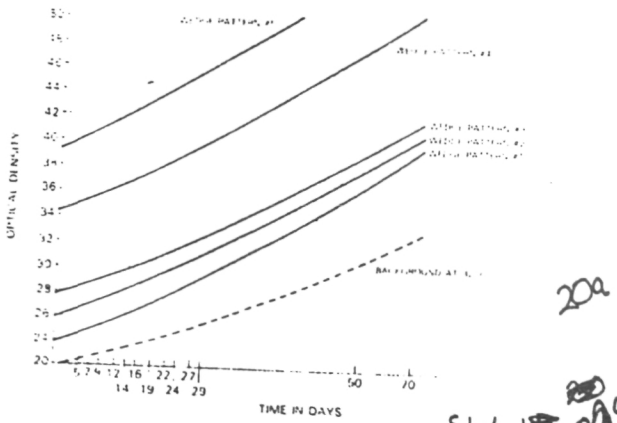


SLIDE 15

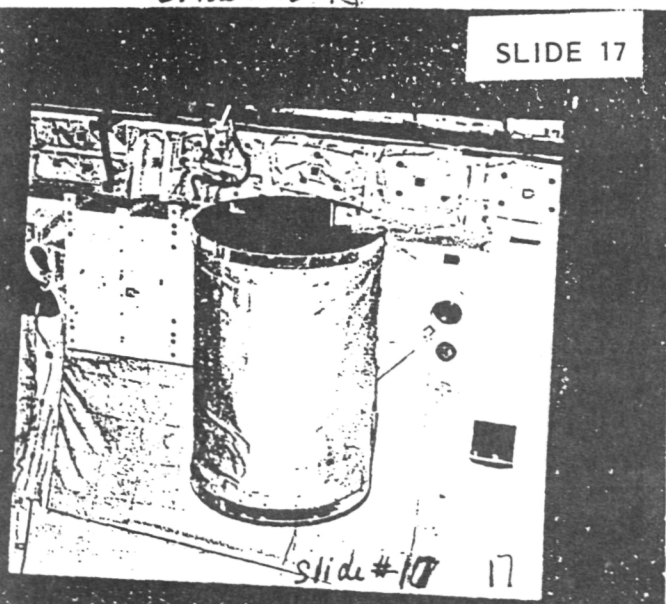


SLIDE 20A

AGING EFFECTS: OPTICAL DENSITY VS. TIME IN DAYS



SLIDE 17



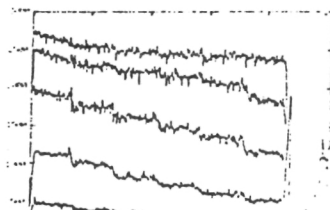
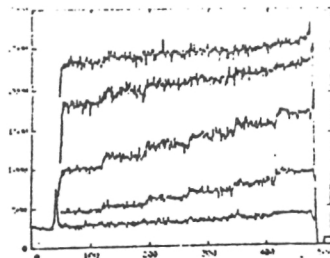
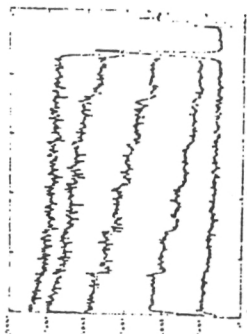
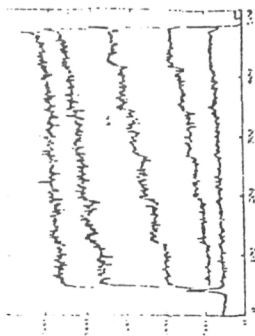
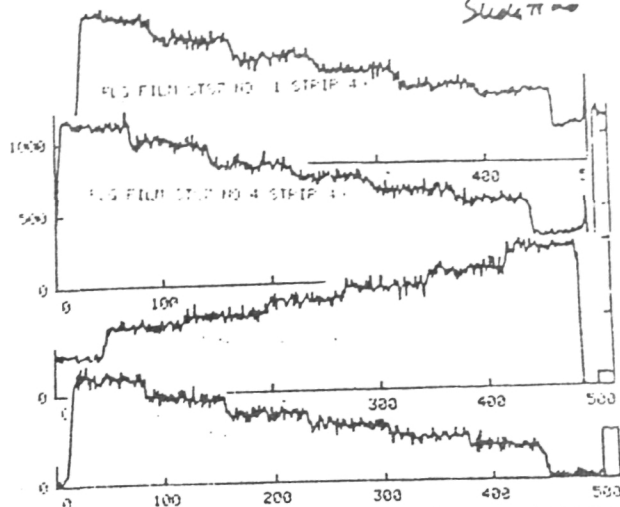
SLIDE 25

ORIGINAL PAGE IS
OF POOR QUALITY

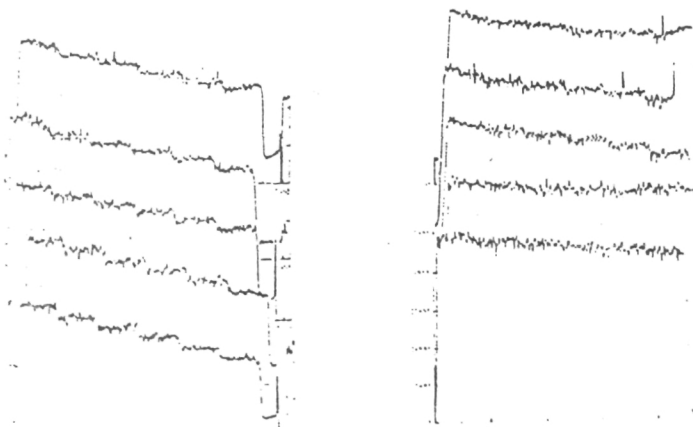
Slide # 25

SLIDE 26

Slide # 26



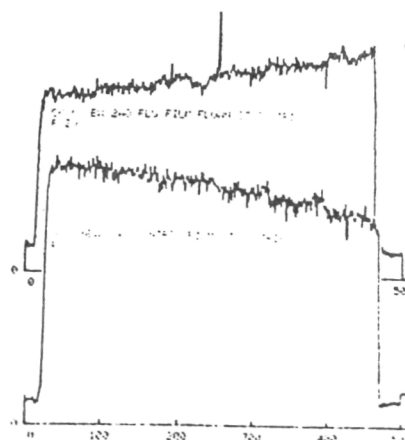
SLIDE 23



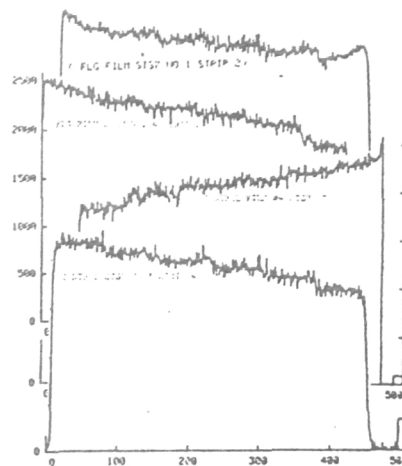
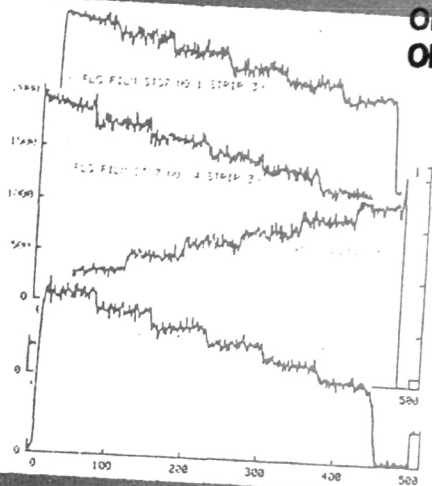
Slide 23

SLIDE 24

Slide # 24
24

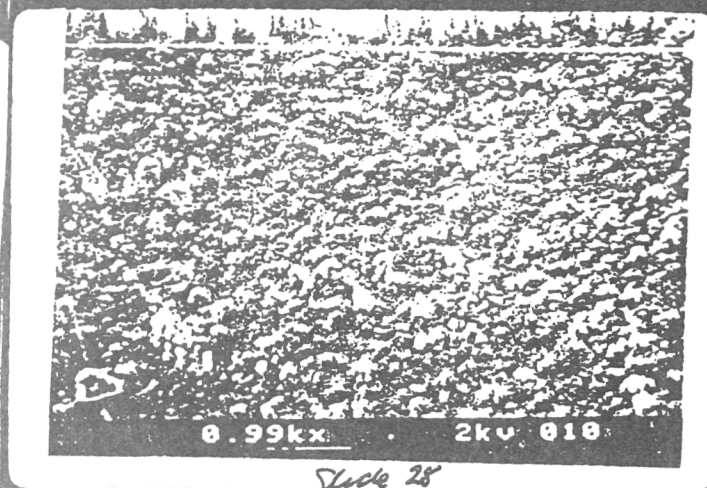
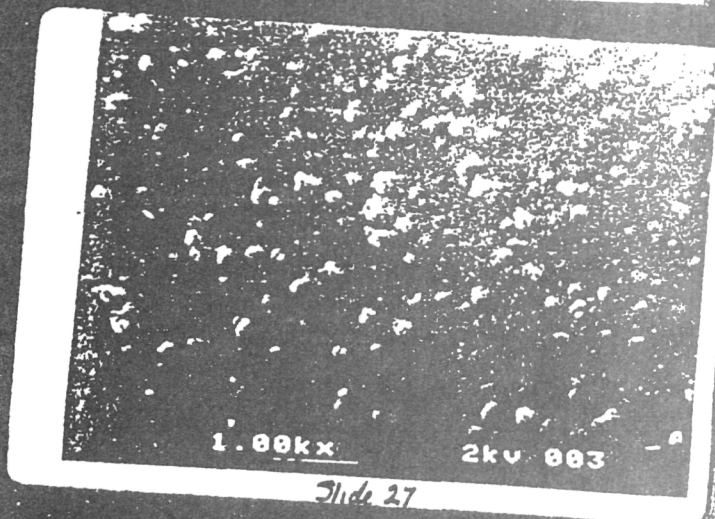


ORIGINAL PAGE IS
OF POOR QUALITY



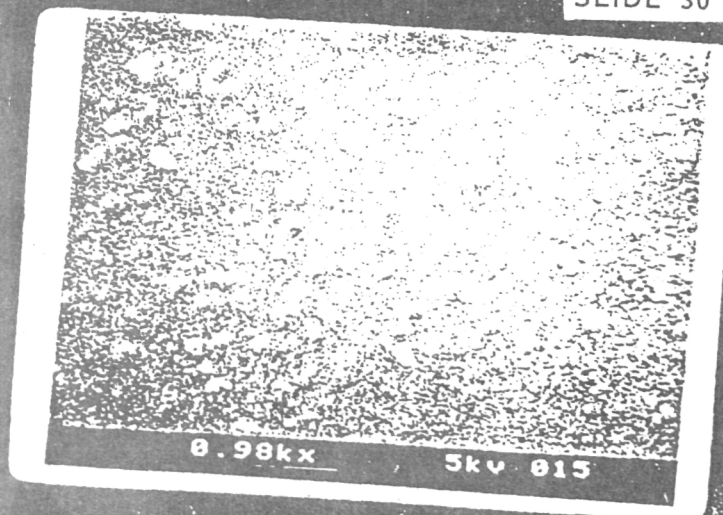
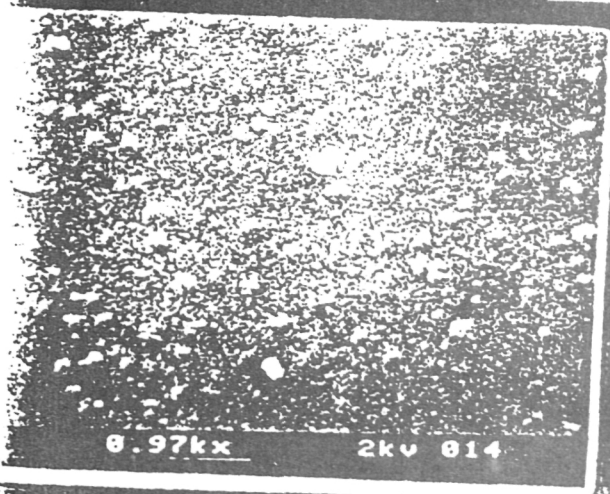
SLIDE 27

SLIDE 28

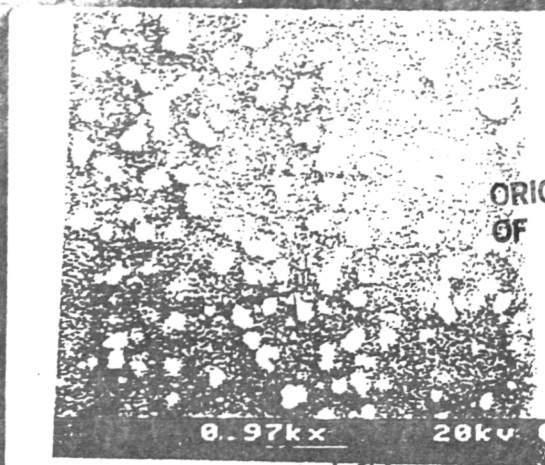


SLIDE 29

SLIDE 30



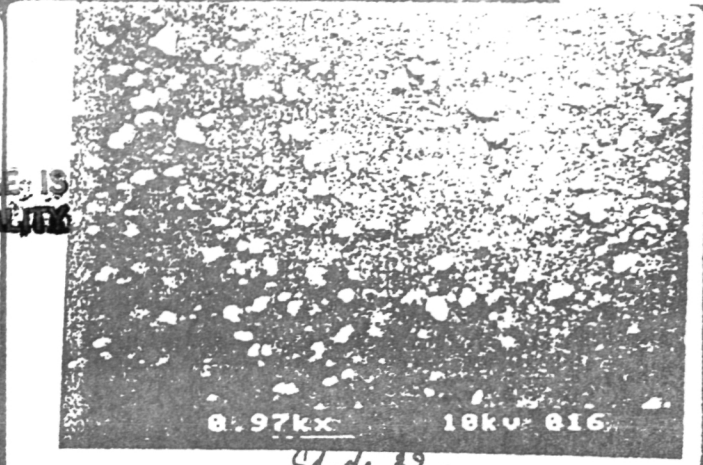
SLIDE 31



Slide 31

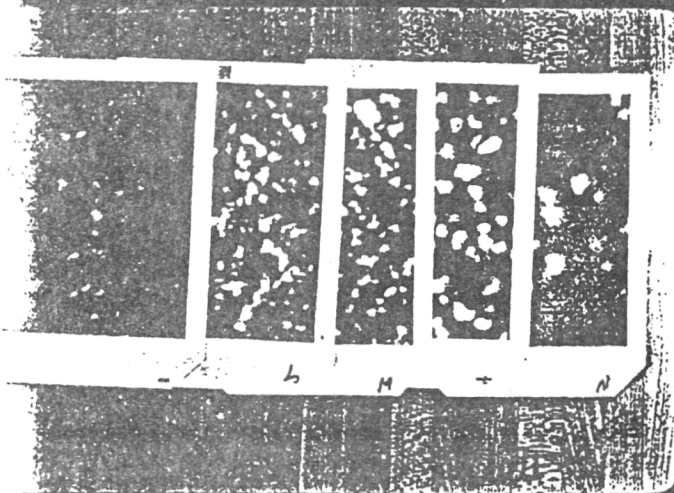
ORIGINAL PAGE IS
OF POOR QUALITY

SLIDE 32

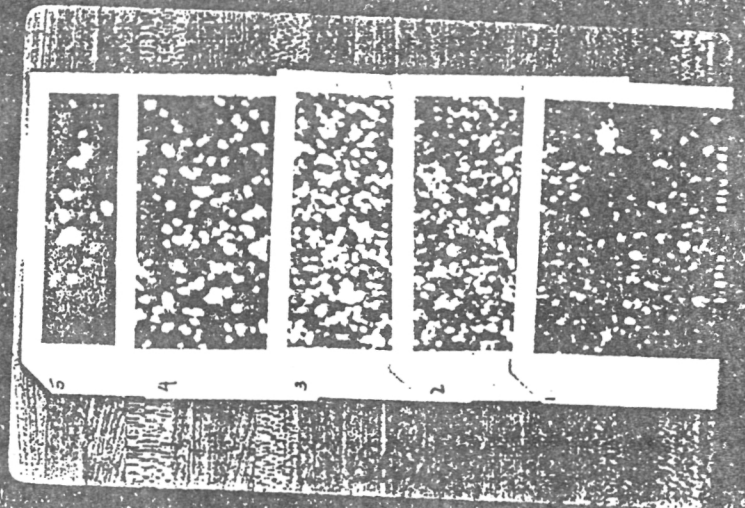


Slide 32

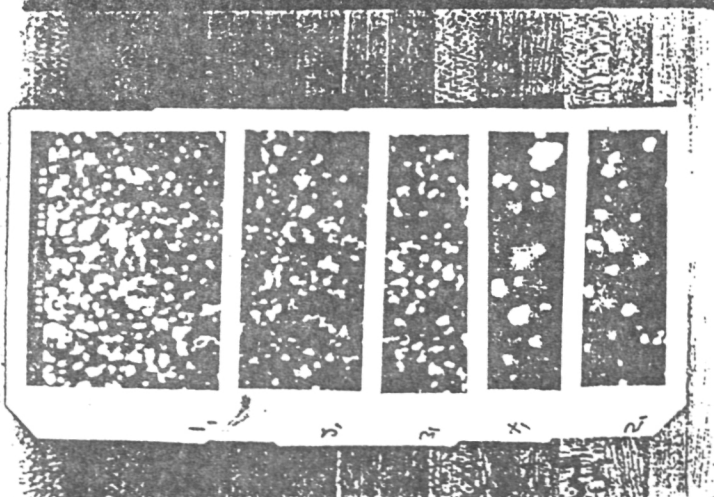
SLIDE 33



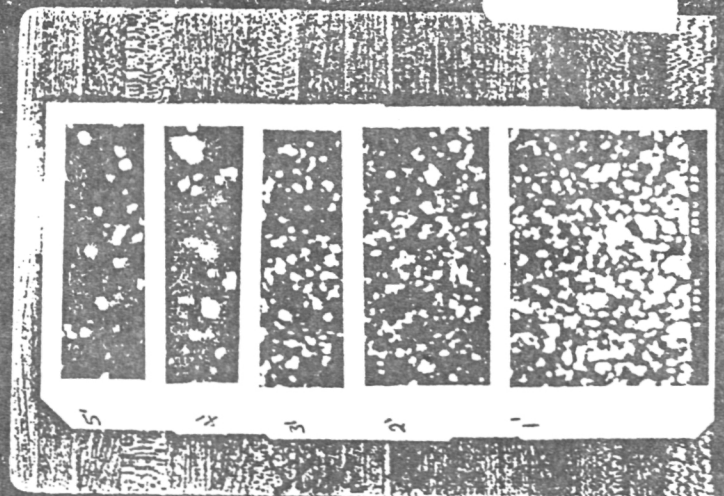
SLIDE 34



SLIDE 35



SLIDE 36



SLIDE 46

ORIGINAL PAGE IS
OF POOR QUALITY

Slide 46

SLIDE 45

Slide 45

SLIDE 44

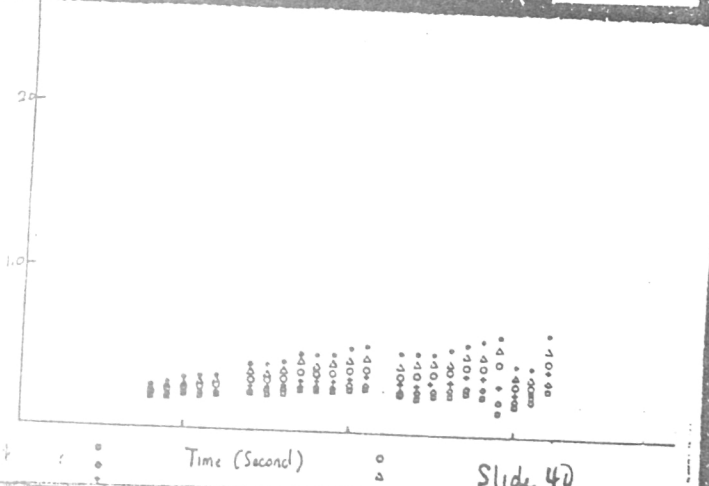
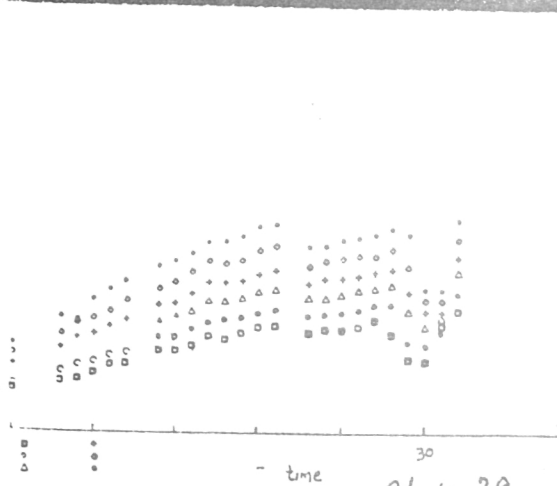
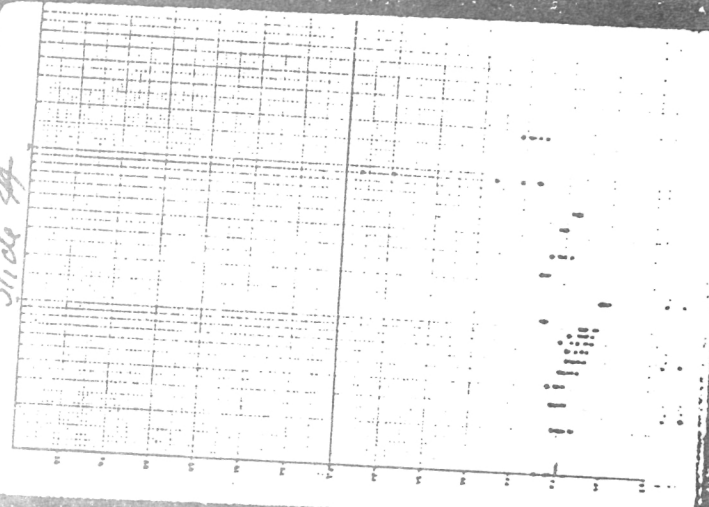
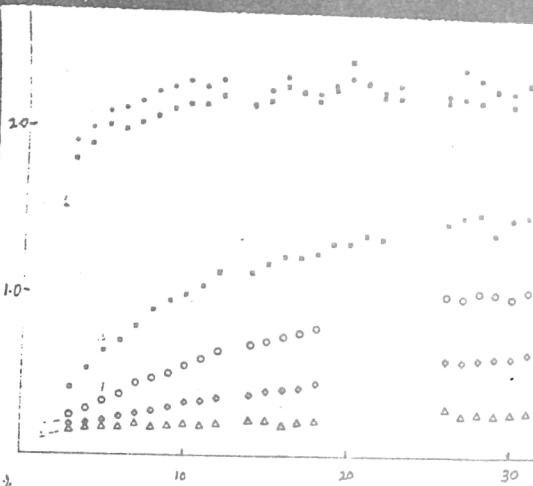
Slide 44

SLIDE 39

SLIDE 40

Slide 39

Slide 40



AVERAGE DENSITY AS FUNCTION OF POSITION ON FILM

Sample	Sample	Sample	Sample
Average	Average	Average	Average
Standard Deviation	Standard Deviation	Standard Deviation	Standard Deviation
Functional Average	Functional Average	Functional Average	Functional Average
Functional Standard Deviation	Functional Standard Deviation	Functional Standard Deviation	Functional Standard Deviation
Sample A, Set I	Sample B, Set I	Sample C, Set I	Sample D, Set I
Average	Average	Average	Average
Standard Deviation	Standard Deviation	Standard Deviation	Standard Deviation
Functional Average	Functional Average	Functional Average	Functional Average
Functional Standard Deviation	Functional Standard Deviation	Functional Standard Deviation	Functional Standard Deviation
Sample A, Set II	Sample B, Set II	Sample C, Set II	Sample D, Set II
Average	Average	Average	Average
Standard Deviation	Standard Deviation	Standard Deviation	Standard Deviation
Functional Average	Functional Average	Functional Average	Functional Average
Functional Standard Deviation	Functional Standard Deviation	Functional Standard Deviation	Functional Standard Deviation

SLIDE 42

Slide 42

Time (seconds)



SLIDE 43

Time (seconds)

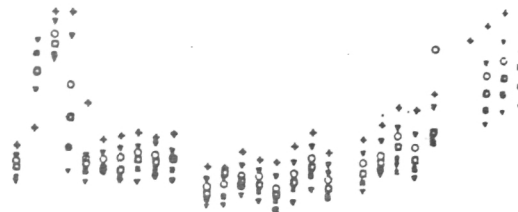
Slide 43



SLIDE 41

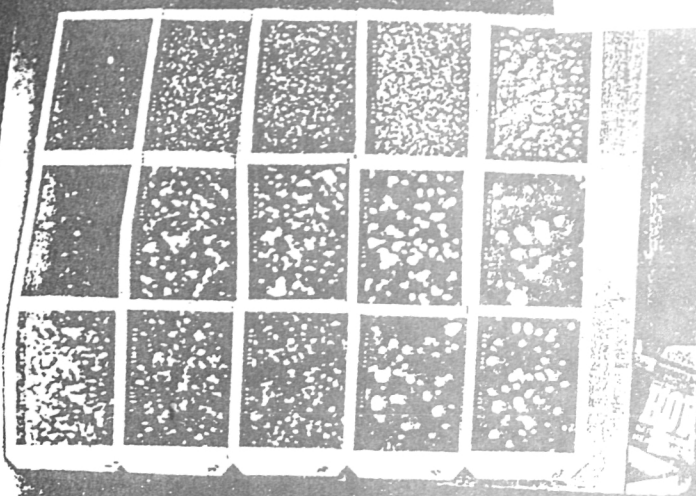
Time (seconds)

Slide 41

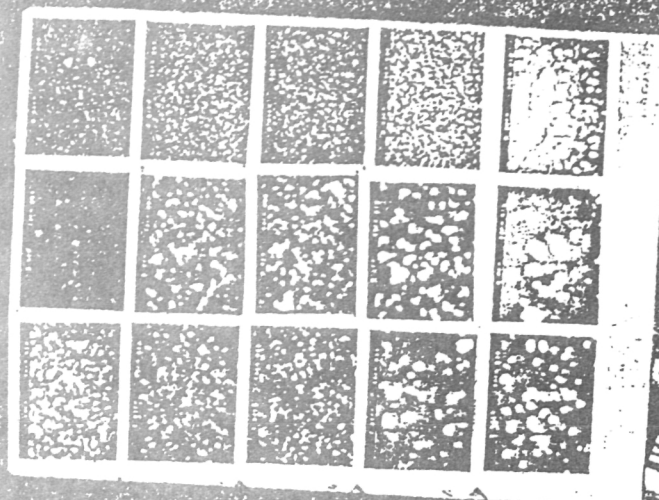


ORIGINAL PAGE IS
OF POOR QUALITY

SLIDE 36B

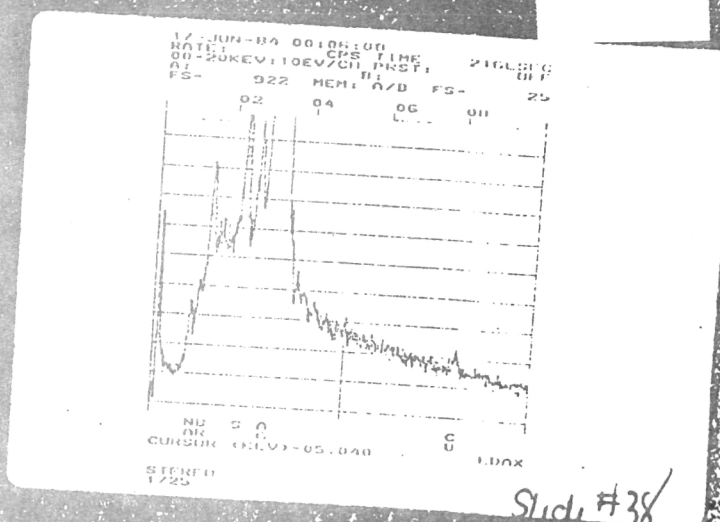
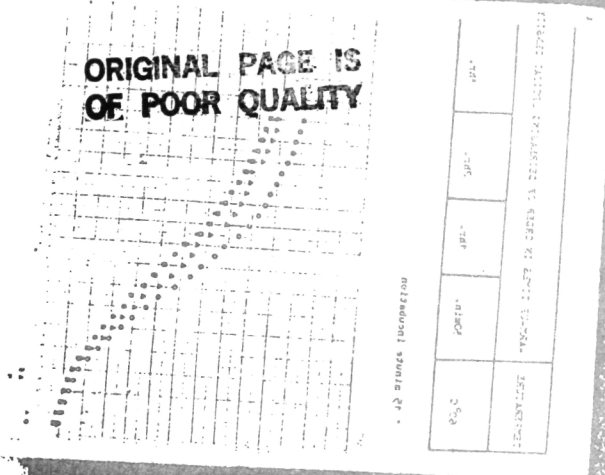


SLIDE 36A



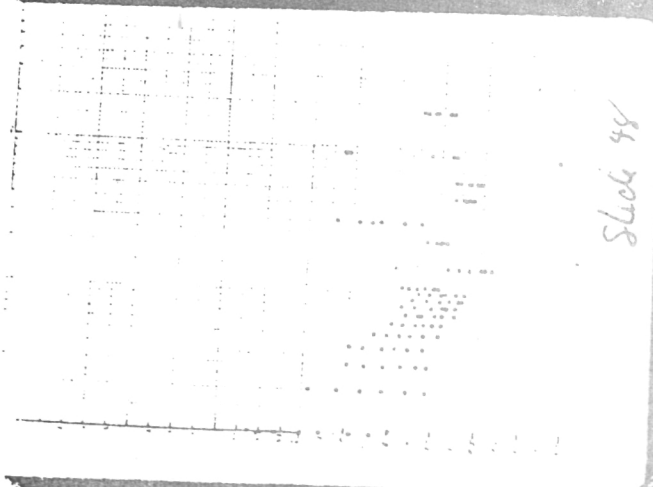
SLIDE 38

ORIGINAL PAGE IS
OF POOR QUALITY



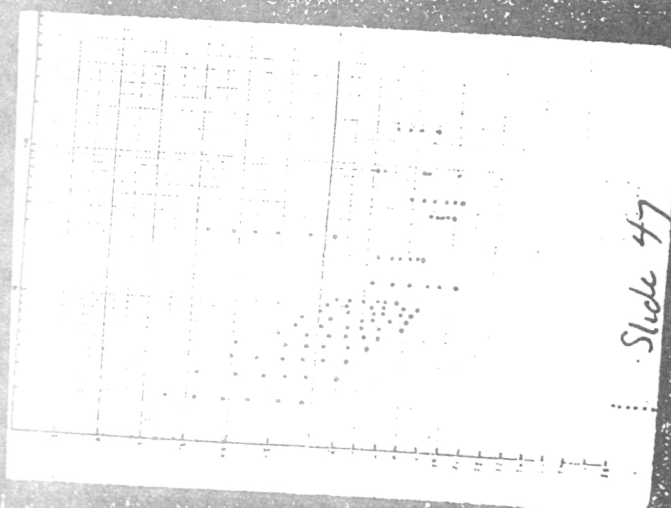
Slide #38

SLIDE 48



Slide 48

SLIDE 47



Slide 47